Available online at www.sciencedirect.com
ScienceDirect
Journal of Catalysis 255 (2008) 1–5
JOURNAL OF CATALYSIS
www.elsevier.com/locate/jcat

Priority Communication

Ceria-catalyzed soot oxidation studied by environmental transmission electron microscopy

S.B. Simonsen [a,b], S. Dahl [a], E. Johnson [b], S. Helveg [a,*]

[a] *Haldor Topsøe A/S, Nymøllevej 55, DK-2800 Kgs. Lyngby, Denmark*
[b] *Nano Science Center, The Niels Bohr Institute, Copenhagen University, Universitetsparken 5, DK-2100 Copenhagen, Denmark*

Received 20 November 2007; revised 10 December 2007; accepted 2 January 2008

Available online 14 February 2008

Abstract

Environmental transmission electron microscopy (ETEM) was used to monitor *in situ* ceria-catalyzed oxidation of soot in relation to diesel engine emission control. From time-lapsed ETEM image series of soot particles in contact with CeO_2, or with Al_2O_3 as inert reference, mechanistic and kinetic insight into the catalytic and noncatalytic oxidation mechanisms was obtained. Specifically, the results indicate that the catalytic soot oxidation mechanism involves reaction centers at the soot–CeO_2 interface and that the interface reaction kinetic properties are in good agreement with previous macroscopic, averaging measurements.

Keywords: Diesel exhausts emission control; Soot oxidation; Ceria-based catalysts; Environmental transmission electron microscopy

1. Introduction

Gasification of carbonaceous matter plays an important role in diverse areas, such as coal conversion and vehicle emission control. Currently, the awareness of soot abatement in the exhaust from diesel engines is increasing due to new environmental legislation for exhaust specifications [1]. Soot removal is accomplished by the introduction of filters on diesel-driven vehicles [1]. An attractive approach to effectively regenerate the filters onboard is to functionalize the filters for catalytic oxidation of the deposited soot [2]. Ceria-based materials are widely adopted for this purpose and have been the subject of several investigations [3–5]. It is generally accepted that the redox properties of CeO_2 are crucial to the catalytic effect, but the detailed reaction mechanism and the location of the catalytic active sites remain matters of debate. For instance, it was proposed that the reaction occurs at the soot–CeO_2 interface [3] and that the reaction occurs through spillover of active oxygen from CeO_2 to reaction centers distributed at the soot surfaces [2,3,6]. Averaging techniques, such as temperature-programmed oxidation and thermogravimetric analysis [2–9], and TEM studies [10], have mainly been used to study the soot oxidation reaction. Although these studies have provided significant insight, previous work on metal-catalyzed gasification of carbonaceous matter emphasized that environmental transmission electron microscopy (ETEM) could be a beneficial complement, due to its capability of providing direct observations at the carbon–catalyst interface *in situ* during the gasification reaction [11–13].

In the present work, ETEM was applied to address the reactions occurring at the soot–ceria interface during exposure to oxidation conditions. Time-lapsed ETEM image series were obtained *in situ* of soot particles in contact with catalytic active CeO_2 or with catalytic inert Al_2O_3 as a reference. The observations reveal that the catalytic oxidation occurred at the soot–CeO_2 interface, whereas noncatalytic combustion was independent of the oxide location. Furthermore, based on ETEM observations at different temperatures, the catalytic interface kinetics was determined and found to be in good agreement with previous findings.

2. Experimental

The experiments were performed on a CM300 FEG TEM (FEI Company) equipped with an environmental cell for *in*

* Corresponding author. Fax: +45 4527 2999.
E-mail address: sth@topsoe.dk (S. Helveg).

0021-9517/$ – see front matter
doi:10.1016/j.jcat.2008.01.004

situ studies [14]. Images and time-lapsed image series (movies) with a resolution of about 0.14 nm of samples during exposure to reactive gases and elevated temperatures can be recorded with this system. To model soot deposited in a diesel particulate filter, a carbon black (CB) powder of particles with a diameter of about 30 nm (Printex U, Degussa GmbH) was mechanically mixed with a CeO_2 catalyst powder, produced as described previously [15], with a volume ratio 1:10. To serve as a reference, the CB was also mixed with α-Al_2O_3 powder in the same ratio. The differences in mass–thickness contrast and morphology facilitated the identification of the CB and oxide particles in the TEM images. Specimens for ETEM experiments were prepared by dispersing a CB-oxide powder over stainless steel TEM grids, which were mounted in the heating holder (Gatan model 628). After being inserted into the TEM instrument, a specimen was exposed to 2 mbar O_2 and heated at 50 °C/min to a reaction temperature in the interval 300–600 °C. Similar experiments were conducted with 2 mbar N_2 as a reference. At a given reaction temperature, images and movies of the CB-oxide samples were recorded using a low-light and fast-scan CCD (Tietz Fastscan F-114). During imaging, the beam current density was kept below 0.16 A/cm^2, which was sufficiently low to avoid influence of the electron beam on the CB particles.

For comparison with the ETEM experiments, CB-oxide samples were oxidized *ex situ* in a separate reactor until approximately half of the CB was combusted. The samples were crushed to obtain tight physical contact between the CB and oxide material. They were oxidized in 2 mbar O_2 in N_2 (1 bar total pressure) in a plug-flow reactor. The progress of the reaction was followed by monitoring the CO and CO_2 levels. A relatively high temperature (600 °C), characteristic for the thermal soot combustion [8], was used for oxidation of the CB–Al_2O_3 mixture. A relatively low temperature (350 °C), characteristic for the catalytic oxidation [8], was used for the CB–CeO_2 mixture. In both cases, the O_2 conversion was below 50%, ensuring that the entire sample was exposed to O_2. After the oxidation reaction, the samples were transferred for conventional TEM (CTEM) investigations on a CM300 FEG microscope (FEI Company).

3. Results and discussion

We first focus on the samples oxidized *ex situ*. Figs. 1a and 1b show CTEM images of an agglomerate of CB particles from the CB–CeO_2 sample before and after oxidation *ex situ*. Apparently, the diameters of the CB particles did not change, even though 50% of the CB was gasified catalytically. In contrast, the noncatalytic oxidized CB–Al_2O_3 sample contained CB particles of a significantly smaller diameter (Fig. 1c). The qualitative observations were corroborated by CB particle size distributions measured from CTEM images (Fig. 1d). These results tentatively suggest that reaction centers could be highly localized for the catalyzed oxidation in the CB–CeO_2 sample and more widely distributed in the CB agglomerates for the thermal combustion in the CB–Al_2O_3 sample. This suggestion is further supported by the observation that the image contrast

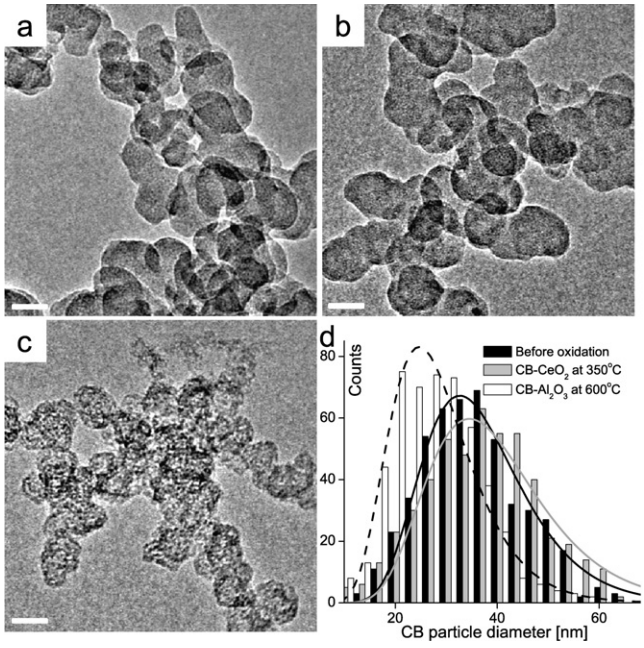

Fig. 1. CTEM images of agglomerates of CB particles. (a) A non-oxidized CB agglomerate (mixed with CeO_2). (b) A CB agglomerate (mixed with CeO_2) after catalytic oxidation *ex situ* at 350 °C. (c) A CB agglomerate (mixed with Al_2O_3) after noncatalytic oxidation *ex situ* at 600 °C. (a)–(c) Scale bars = 30 nm. (d) Particle size distributions of CB particles (including 500 counts each). The particle size is determined as the diameter in a circular approximation to the projected area of the soot particles. To guide the eye, a lognormal distribution function is fitted to each histogram.

of CB particles was unaltered in the CB–CeO_2 sample but became more granulated for the CB particles in the CB–Al_2O_3 sample (Figs. 1a and 1c).

To address the role of the CeO_2 catalyst, ETEM experiments were performed to monitor agglomerates of CB particles attached to CeO_2 particles *in situ* during exposure to oxygen at elevated temperatures. The time-lapsed series of ETEM images show the main findings (Fig. 2, see also supplementary material): The images reveal that agglomerates of CB particles moved toward the CeO_2 and vanished (Figs. 2a–2c), whereas agglomerates of CB particles did not protrude and move away from the edges of the CeO_2 particles. These findings suggest that the motion was related not only to the migration of CB along the CeO_2 surface, but also to the oxidizing reaction conditions. This finding is consistent with results of similar experiments using N_2 instead of O_2, in which ETEM image series showed that CB particle agglomerates remained stable. Moreover, monitoring the CB–Al_2O_3 samples by ETEM during exposure to the oxidizing conditions (Figs. 2d–2f) show that the agglomerates of CB particles were stable at the same temperature and over the same time period. Thus, the findings indicate that the CeO_2 catalyzed oxidation of the CB agglomerates and concurrently generated motion of the agglomerates toward the catalyst surface.

In an analysis of the ETEM observations, the CB particle diameters and positions relative to CeO_2 were mapped out in consecutive images as outlined in Figs. 3a and 3b. Fig. 3c shows the results for two CB particles during oxidation at 500 °C. Clearly, the relative projected distances in the images between the CB

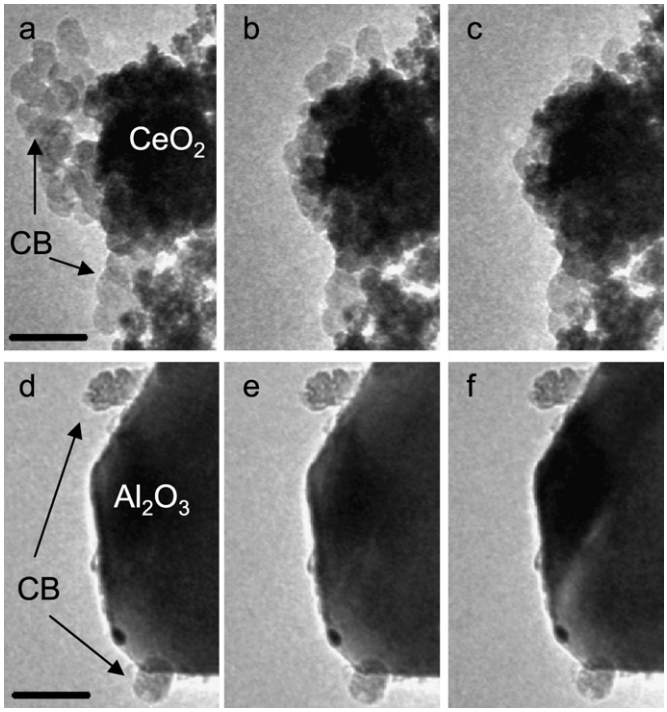

Fig. 2. Time-lapsed ETEM images of (a–c) CB–CeO_2 and (d–f) CB–Al_2O_3 recorded during exposure to 2 mbar O_2 at 550 °C. The time interval between each image is ∼2 min. Scale bars = 90 nm.

particles and the CeO_2 shrank linearly with time; thus, because the periphery of the agglomerate also remained constant with time, the CB particles had to move at constant velocity toward the CeO_2. Furthermore, in the corresponding time interval in which the CB particles moved over projected distances comparable to their diameter, the CB particle diameters remained constant. These findings indicate that carbon was oxidized by the ceria catalyst only when carbon was situated in close proximity of the CB–CeO_2 interface, and thus the catalytic reaction mechanism involved reaction centers near the CB–CeO_2 interface. Based on these observations, we are able to pinpoint the reactive interface down to only a few nanometers due to the projection geometry (overlap of CeO_2 and CB) in the images and the roughness of the CeO_2 surface. The findings that the catalytic effect was localized at the CB–CeO_2 interface are also consistent with the observation that the CB particle size distribution was unaltered by *ex situ* catalytic oxidation. Moreover, many CB agglomerates were observed with a constant periphery in the projected ETEM images, reflecting a constant linear motion toward CeO_2. However, agglomerates were also observed with the periphery changing over time. A change in periphery can be explained by a rotation with respect to an axis in the image plane; thus, we attribute such observations to CB agglomerates which moved toward and concurrently rotated around the CeO_2 to which the agglomerates were attached. The present analysis includes only agglomerates that apparently moved linearly toward the ceria.

Next, we address the question of whether the interface reaction sufficiently explains the catalytic role of CeO_2 by considering the kinetics associated with the CB–CeO_2 interface

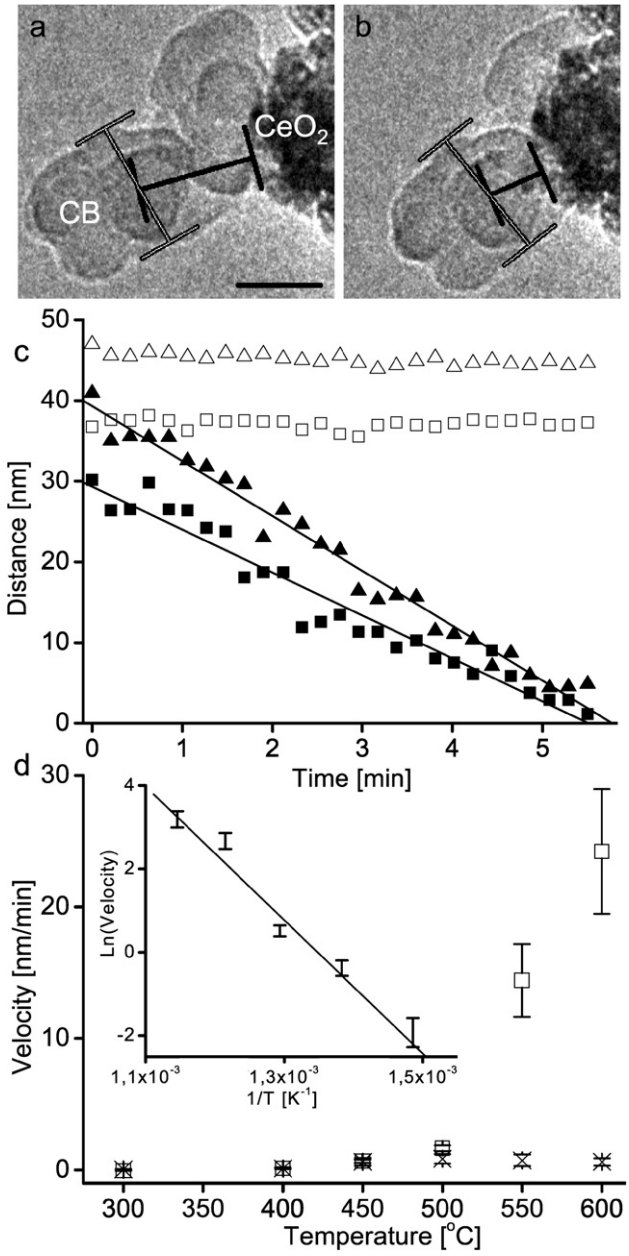

Fig. 3. (a and b) ETEM images of CB–CeO_2 during exposure to 2 mbar O_2 at 500 °C (extracted from the ETEM movie in supplementary material). Scale bar = 30 nm. The time interval between the images is ∼12 min. The measured diameter (white line) and projected CB–CeO_2 distance (black line) are marked. The estimated accuracy on the diameter and the distance is 0.5 nm and 0.9 nm, respectively. (c) Diameters (open symbols) of two different CB particles and distances from the particle centers to the catalyst edge (filled symbols) as a function of time during exposure to 2 mbar O_2 at 500 °C. (d) Average projected speed of CB relative to CeO_2 (□) and Al_2O_3 (×) presented for different temperatures. For each temperature, the average speed and the standard deviation are obtained from observations of 10 particles in different agglomerates. The insert presents an Arrhenius plot of the dataset.

reaction. To probe the reaction kinetics, ETEM experiments at different reaction temperatures in the interval 300–600 °C were conducted. The ETEM image series at different temperatures show qualitatively the same behavior as illustrated in Fig. 2. In these experiments, the projected velocity of the CB agglomerates toward the CeO_2 surface was determined from

the difference in the CB position relative to the CeO_2 in two consecutive images recorded with the electron beam switched off in the intervening time interval to further ensure that the effect of the beam was negligible. At each reaction temperature, an average velocity of the CB agglomerates was determined from the observations of 10 different agglomerates. The average velocity was found to increase with temperature, as shown in Fig. 3d. Assuming that the interface reaction rate was proportional to the projected velocity of the CB agglomerates, an apparent activation energy barrier for the CeO_2-catalyzed CB oxidation could be obtained from an Arrhenius analysis of the data in Fig. 3d. From this analysis, an activation energy barrier of $E_a = (133 \pm 7)$ kJ/mol was obtained, in agreement with previously reported values [3–5]. In previous investigations using averaging techniques, the activation energy is often found to depend on the degree of physical contact between the soot particles and the catalyst in such a way that "tight" contact mixtures usually resulted in lower activation energy barriers than "loose" contact mixtures [7]. The ETEM-based value for the apparent activation energy agrees better with the previously reported values for "tight" mixtures. This is expected because the ETEM is able to monitor those CB agglomerates only in direct physical contact with catalyst particles.

In comparison, similar ETEM measurements of the relative velocity of CB in contact with Al_2O_3 show that the CB agglomerates did not move significantly relative to the Al_2O_3 even at the highest temperatures (Fig. 3d), emphasizing the importance of the interface reaction for the CeO_2 catalyst. At the highest reaction temperatures of 550–600 °C, the CB particles tended to shrink in diameter, suggesting that the noncatalytic combustion of the CB obtained a more significant reaction rate, in accordance with previous studies [5,8] and with the particle size distributions after oxidation *ex situ* (Fig. 1c). The shrinkage rate was determined by monitoring the CB particle diameters over time at 550 °C. This analysis shows that the CB shrinkage rate was <5% of the mean projected velocity of CB toward CeO_2 and that this result could be extrapolated to temperatures up to 600 °C. Thus, motion of CB due to the shrinkage of the CB particles located closer to the CeO_2 surface is of minor importance.

The direct observations suggest that the catalytic effect is related to interface processes and shows that the CB–CeO_2 interface apparently can be continuously reestablished over the course of the reaction. This is interesting because it is noted that the activity of catalytic soot oxidation decreases over time and that this is explained as loss in contact area between soot and catalyst [8]. This scenario may seem to be in contrast with the present ETEM findings; however, in particulate filters, the size and distribution of soot particles and catalyst may differ from the present model samples, and the soot particles may be part of a larger network (e.g., a soot cake). In such configurations, other phenomena may play additional roles; for instance, a competition may prevail between reestablishing the soot–catalyst interface and bonding the soot agglomerate to the soot network. Thus, the soot–catalyst interface may break up, in which case soot transport to the catalyst surface will be rate-determining.

Finally, we briefly turn to the origin of the reactions at the CB–CeO_2 interface. The ETEM observations indicate that CB was removed from the interface. This removal of CB most likely occurred through reaction with oxygen in the ceria surfaces to form CO_2 or CO. It may be speculated that oxidation leaves empty sites at the solid–solid interface; if this were the case, attractive van der Waals forces between CB and CeO_2 could be responsible for reestablishing the interface. However, the oxidation reaction may also proceed without creating empty interface sites. Such a process could be mediated by surface transport and restructuring of soot or ceria, comparable to the reaction dynamics revealed for catalytic graphene growth [16]. Recently, based on kinetic arguments, a catalytic reaction mechanism was proposed to involve spillover of adsorbed oxygen from the catalyst to the CB, followed by diffusion over the CB surface and finally CB oxidation at active sites at the CB particle [6]. This mechanism is also consistent with the present ETEM results as long as the active sites at the CB particle are located within a few nanometers from the CB–CeO_2 interface. In the present experiments, the apparent overlap of CeO_2 with CB particles in the projected ETEM images hamper resolution of the interface processes beyond this limit. Further insight into the atomic-scale reaction mechanism in the ceria-catalyzed soot oxidation may be gained only by more detailed *in situ* investigations.

4. Conclusion

In the present study, ETEM was used to obtain *in situ* observations of CeO_2-catalyzed soot oxidation at the nanoscale. The results show that the catalytic oxidation reaction involved processes, which were confined to the soot–CeO_2 interface region, and the catalytic reaction resulted in motion of soot agglomerates toward the catalyst surface, which acted to reestablish the soot–CeO_2 interface in the course of the oxidation process. This work further demonstrates that the apparent activation energy of CeO_2-catalyzed soot oxidation could be measured by using ETEM for a better-defined tight physical contact situation. The observed reaction dynamics is consistent with the observations from *ex situ* oxidation experiments and is quantitatively in a good agreement with previous kinetic investigations.

Acknowledgments

We gratefully acknowledge the participation of the CTCI Foundation, Taiwan, in the establishment of the ETEM facility at Haldor Topsøe A/S. E. Johnson acknowledges support from the Danish Natural Science Research Council.

Supplementary material

ETEM movie of CB–CeO_2 during exposure to 2 mbar O_2 at 500 °C. The frames were recorded consecutively with an exposure time of 0.5 s and a waiting time of 12.0 s. In this movie the frames are displayed at a rate of 10 frames/s.

Please visit DOI: 10.1016/j.jcat.2008.01.004.

References

[1] B.A.A.L. van Setten, M. Makkee, J.A. Moulijn, Catal. Rev. 43 (2001) 489.
[2] A.G. Konstandopoulos, E. Papaionannou, D. Zarvalis, S. Skopa, P. Baltzopoulou, E. Kladopoulou, M. Kostoglou, S. Lorentzou, SAE Tech. Paper (2005) no. 2005-01-0670.
[3] B. Dernaika, D.A. Uner, Appl. Catal. B 40 (2003) 219.
[4] M.N. Bokova, C. Decarne, E. Abi-Aad, A.N. Pryakhin, V.V. Lunin, A. Aboukaïs, Thermochim. Acta 428 (2005) 165.
[5] X. Wu, D. Liu, K. Li, J. Li, D. Weng, Catal. Commun. 8 (2007) 1274.
[6] K. Krishna, A. Bueno-López, M. Makkee, J.A. Moulijn, Appl. Catal. B 75 (2007) 189.
[7] B.A.A.L. van Setten, J.M. Schouten, M. Makkee, J.A. Moulijn, Appl. Catal. B 28 (2000) 253.
[8] P. Darcy, P. Costa, H. da Mellottee, J.M. Trichard, G. Djega-Mariadassou, Catal. Today 119 (2007) 52.
[9] J.P.A. Neeft, T.X. Nijhuis, E. Smakman, M. Makkee, J.A. Moulijn, Fuel 76 (1997) 1129.
[10] H. Jung, D.B. Kittelson, M.R. Zachariah, Combust. Flame 136 (2004) 445.
[11] R.T.K. Baker, Catal. Rev. Sci. Eng. 19 (1979) 161.
[12] R.T.K. Baker, J.A. France, L. Rouse, R.J. Waite, J. Catal. 41 (1976) 22.
[13] R.J. Liu, P.A. Crozier, C.M. Smith, D.A. Hucul, J. Blackson, G. Salaita, Appl. Catal. A 282 (2005) 111.
[14] P.L. Hansen, A.K. Datye, S. Helveg, Adv. Catal. 50 (2006) 77.
[15] B. Djuricic, S. Pickering, J. Eur. Ceram. Soc. 19 (1999) 1925.
[16] S. Helveg, C. Lopez-Cartes, J. Sehested, P.L. Hansen, B.S. Clausen, J.R. Rostrup-Nielsen, F. Abild-Pedersen, J.K. Nørskov, Nature 427 (2004) 427.